7-2012

Guided wave signal transport in curved and tapered plates

Ronald A. Roberts
Iowa State University, rroberts@iastate.edu

Guided wave signal transport in curved and tapered plates

Abstract
A numerical study is presented of the influence of plate curvature and taper on the transport of ultrasound guided wave signals for nondestructive evaluation (NDE) and structural health monitoring (SHM) applications. Model formulations for transmission at sharp transitions in plate curvature and thickness taper are summarized. Results are presented showing that transitions in plate curvature and tapered plate thickness have minimal effect on signal transmission efficiency when associated characteristic dimensions are large compared to plate thickness.

Keywords
acoustic signal processing, plates (structures), structural acoustics, ultrasonic transmission, nondestructive evaluation, QNDE

Disciplines
Materials Science and Engineering

This article appeared in *AIP Conference Proceedings* 1511 (2012): 121–128 and may be found at http://dx.doi.org/10.1063/1.4789039.

Guided wave signal transport in curved and tapered plates

R. A. Roberts

Citation: AIP Conf. Proc. **1511**, 121 (2013); doi: 10.1063/1.4789039
View online: http://dx.doi.org/10.1063/1.4789039
View Table of Contents: http://proceedings.aip.org/dbt/dbt.jsp?KEY=APCPCS&Volume=1511&Issue=1
Published by the American Institute of Physics.

GUIDED WAVE SIGNAL TRANSPORT IN CURVED AND TAPERED PLATES

R. A. Roberts
Center for NDE, Iowa State University, Ames, IA 50014

ABSTRACT. A numerical study is presented of the influence of plate curvature and taper on the transport of ultrasound guided wave signals for nondestructive evaluation (NDE) and structural health monitoring (SHM) applications. Model formulations for transmission at sharp transitions in plate curvature and thickness taper are summarized. Results are presented showing that transitions in plate curvature and tapered plate thickness have minimal effect on signal transmission efficiency when associated characteristic dimensions are large compared to plate thickness.

Keywords: Ultrasound, Guided Waves
PACS: 43.35.Yb 43.35.Zc 43.38.Hz

INTRODUCTION

Ultrasonic measurements for nondestructive evaluation (NDE) and structural health monitoring (SHM) of airframe structures often involve the transport of ultrasonic signals as guided wave modes in plate structures. Efforts in development of guided wave measurements for NDE and SHM applications are by-and-large carried out using uniformly thick planar plate test structures, in which guided wave propagation occurs in the form of truly independent modes of motion, i.e., motion that propagates through the plate without energy loss or conversion into other possible modes of propagation. Actual airframe structures consist of non-planar plate geometries displaying non-uniform thickness. It is prudent therefore to ask what influence these non-ideal geometric attributes have on the transmission of guided wave signals. A computational study was therefore undertaken to quantitatively explore the influence curvature and thickness taper on guided wave signal propagation. The study examined a set of canonical non-ideal plate geometries, in order of increasing complexity. Initial activity examined the propagation characteristics of circular cylindrical shells, the simplest of non-planar shell geometries. Work next examined guided wave transmission between joined circular shell sections of different radii, which forms the basis of an effective approach to model propagation in generally curved uniformly thick plates. Lastly, work studied the introduction of taper in plate thickness. Interest in this study is in plate curvature having curvature radii much larger than the thickness of the plate. Similarly, interest is in gradual tapers of plate thickness, occurring over lengths substantially greater than the thickness of the plate. Generally speaking, it was observed in this study that variation in plate curvature and thickness of this type has minimal influence on the transmission of guided wave energy.

The 39th Annual Review of Progress in Quantitative Nondestructive Evaluation
AIP Conf. Proc. 1511, 121-128 (2013); doi: 10.1063/1.4789039

MODEL FORMULATION

The canonical problem by-and-large underlying NDE/SHM technology is guided wave propagation in a homogeneous linearly elastic plate having infinite planar parallel traction-free surfaces. Application of linear elastodynamic theory to this configuration reveals the existence of independent modes of propagation which traverse the structure freely, without loss of energy or conversion into alternate modes of propagation.[1] Modes of motion in the planar plate are characterized by either symmetry or asymmetry about the plate mid-plane. Propagating modes are correspondingly denoted A0, S0, A1, S1, etc., where A and S denote asymmetric and symmetric motions, respectively, and the numerical designation indicates order of emergence from evanescent to propagating with increasing temporal frequency. Similarly, the case of a circular cylindrical shell of uniform thickness can be modeled by a straightforward analysis.[2] As with the flat plate, guided wave propagation is revealed to consist of freely propagating modes of motion, which correspond precisely to those in the flat plate as the cylinder radius becomes large.

To examine more general plate geometries, principles of elastodynamic reciprocity are applied.[3] This formulation leads to a boundary integral expression relating displacements $u_i(x)$ and tractions $\tau_{ij}(x)$ over the bounding surface of a body, in terms of the response of an associated canonical geometry to an applied point load

$$\int_B (u_i(x)\,\tau^G_{ij:k}(x\,|\,x') - u^G_{i:k}(x\,|\,x')\,\tau_{ij}(x))\,n_j(x)\,dx + \tfrac{1}{2}\,u_k(x') = 0 \quad , x' \text{ on } B \qquad (1)$$

where displacements $u_i^G(x|x')$ and tractions $\tau_{ij}^G(x|x')$ are the canonical Green state responses to a point load applied at position x'. It is assumed in writing Eq.(1) that the boundary B of the plate structure has a continuously varying normal vector at x', and that the integral is interpreted in the principal value sense at x'. Time harmonic motion is assumed in deriving Eq.(1), and the dependence of all field quantities on frequency ω is implicitly assumed. Wave motions are restricted in this study to two Cartesian dimensions, implying that all plate geometries and wave fields display no dependence upon the x_3 direction. Appropriate specification of boundary conditions in Eq.(1) leads to an integral equation governing wave motion in the geometry of interest.

An integral equation expressed as Eq.(1) is solved numerically using the boundary element method (BEM). In this approach, the sought field quantities are represented by weighted sums of appropriate functions (e.g. piecewise polynomials) prescribed over the boundary of the body (boundary elements). Use of these field representations in Eq.(1) results in a matrix equation for the weighting coefficients (boundary element matrix), where the matrix coefficients are evaluated through numerical integration. A well conditioned matrix is obtained by evaluating Eq.(1) at points x' judiciously positioned over the boundary surface. The accuracy of the BEM computation is monitored by examining the balance between incident and transmitted/reflected energy. The fineness with which boundary surfaces are divided into boundary elements is established by summing total energy carried by all transmitted and reflected propagating modes. Element refinement is prescribed to assure that the sum of reflected and transmitted energies equals the energy carried by the incident wave to within one percent.

The problem representing the next level of complexity beyond the circular shell to which Eq.(1) is applied is transmission of a guided wave at the junction between two cylindrical shells having different radii. To address this problem, the Green function employed in Eq.(1) is the response to a point load acting in a circular cylindrical shell. To

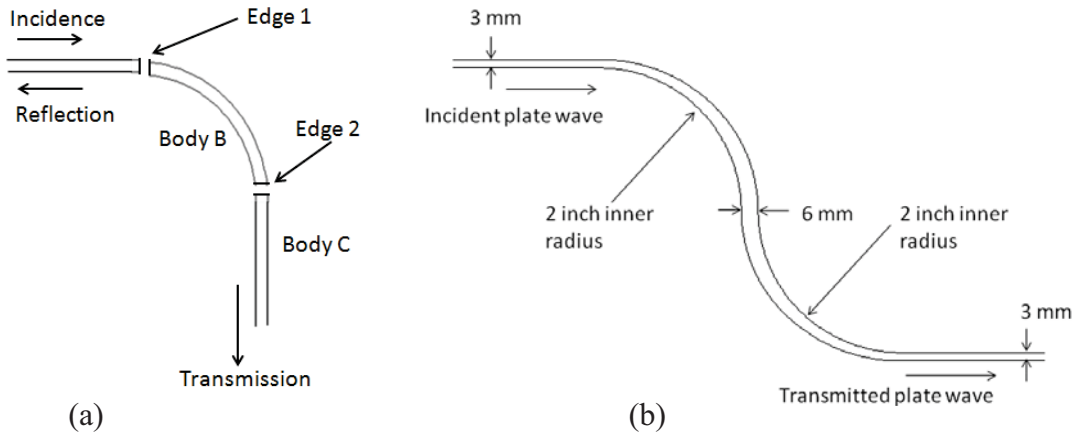

FIGURE 1. Problem configurations: transmission at a) circular curved section, b) tapered section.

facilitate the examination of guided wave transmission, the Green function is derived in non-periodic form following the methods of Felsen.[4] Using this formulation, a Green function is derived which satisfies traction free boundary conditions over an angular section of shell, and transitions naturally to the corresponding Green function for an infinite plate when the shell radius becomes large. The satisfaction of traction free boundary conditions by the Green function on the shell surfaces serves to reduce the support of the integral equation to the surfaces joining the shell sections. An example of application is depicted in Fig.(1a), which considers transmission between three shell sections: two flat semi-infinite plates (infinite radius), and a 90 degree section of circular shell of corresponding thickness. An incident guided wave $u_i^{inc}(x)$ propagates towards the curved section in the left semi-infinite plate, and transmitted and reflected guided mode amplitudes are sought in the bottom and left plate sections, respectively. Three coupled integral equations are obtained by applying Eq.(1) to each shell section in Fig.(1a). The radiation condition at infinity is applied to reflected and transmitted fields in the semi-infinite plates. Additionally, Eq.(1) is applied to the incident field in the semi-infinite plate section which complements the left plate section in Fig.(1a), along with the radiation condition at infinity. The Green function for an infinite flat plate is used in the boundary integral equations for the semi-infinite plates. The Green function for the circular cylindrical shell is used in the boundary integral equation for the circular shell section. The inherent satisfaction of the traction free boundary conditions on the shell surfaces leads to a system of three equations, involving integrations over the edges E_1 and E_2 of the shell sections at which the sections are joined

$$\int_{E_1} (u_i(x)\,\tau^{GP}_{ij:k}(x\,|\,x') - u^{GP}_{i:k}(x\,|\,x')\,\tau_{ij}(x))\,n^A_j(x)\,dx + \tfrac{1}{2}\,u_k(x') = u^{inc}_k(x'),\ x' \text{ on } E_1$$

$$\int_{E_1+E_2} (u_i(x)\,\tau^{GC}_{ij:k}(x\,|\,x') - u^{GC}_{i:k}(x\,|\,x')\,\tau_{ij}(x))\,n^B_j(x)\,dx + \tfrac{1}{2}\,u_k(x') = 0,\ x' \text{ on } E_1 \text{ or } E_2 \quad (2)$$

$$\int_{E_2} (u_i(x)\,\tau^{GP}_{ij:k}(x\,|\,x') - u^{GP}_{i:k}(x\,|\,x')\,\tau_{ij}(x))\,n^C_j(x)\,dx + \tfrac{1}{2}\,u_k(x') = 0,\ x' \text{ on } E_2$$

where $\tau_{ij}^{GP}(x|x')$ is the Green function stress response to a point load acting in a planar infinite plate, $\tau_{ij}^{GC}(x|x')$ is the Green function stress response to a point load acting in a circular cylindrical shell, and n_j^A, n_j^B, and n_j^C are the outward normal vectors for the three constituent bodies. Application of the boundary element method leads to a matrix equation for the evaluation of the displacements $u_i(x)$ and tractions $\tau_{ij}(x)\,n_j$ on the plate edges E_1 and E_2. Following computation of the wave fields on the plate edges, transmitted and reflected

field amplitudes are obtained by application of Eq.(1) to the bottom and left semi-infinite plates, respectively, with the point source position x' placed at a large distance from the plate edge. In this configuration, the Green function response $u_i^{GP}(x|x')$, $\tau_{ij}^{GP}(x|x')$ can be evaluated asymptotically for large |x-x'|, and is found to be dominated by a sum of terms $u_i^{GPm}(x|x')$, $\tau_{ij}^{GPm}(x|x')$ representing the individual propagating guided modes. The amplitude of a specific transmitted or reflected mode m is obtained by integrating the corresponding term of the Green function far-field expression over the plate edge

$$u_k^m(x') = \int_{E_n} (u_i(x)\, \tau_{ij:k}^{GPm}(x \mid x') - u_{i:k}^{GPm}(x \mid x')\, \tau_{ij}(x))\; n_j(x)\, dx\,, \; x' \to \infty \tag{3}$$

where $u_k^m(x')$ is the displacement associated with mode type m=A0, S0, etc.. Reflected modes are obtained by integrating over edge E_1 with x' positioned at large distance in the left semi-infinite plate section, whereas transmitted modes involve integration over edge E_2 with x' positioned at large distance in the bottom semi-infinite plate section.

Guided mode propagation in plates displaying tapered thickness is modeled by applying Eq.(1) using the Green function response for an unbounded space. This formulation is applicable to any geometry without restriction, and is the basis of previous work examining guided plate wave transmission at anomalous features such as joints, corners, and attachments.[5] However, this generality comes at a computational cost. Because the Green function for the unbounded medium does not satisfy traction free boundary conditions, the displacements must be explicitly determined everywhere on the surface of the shell section, resulting in a large BEM matrix. A curved tapered plate structure, shown in Fig.(1b), is segmented into a curved tapered section joining two semi-infinite plates, and Eq.(1) is applied to each section. Application of Eq.(1) to the semi-infinite plate sections proceeds as previously discussed, where the Green function response for an infinite planar plate is employed, along with imposition of radiation conditions at infinity. Application of Eq.(1) to the curved tapered section employs the Green function response for an infinite medium. As before, an incident plate mode is assumed in the left semi-infinite plate. Incorporation of the incident mode as input data into the system of integral equations is accomplished by applying Eq.(1) to the complement of the semi-infinite plate from which the incident mode emerges. Results are then combined to form a system of integral equations expressed as

$$\begin{aligned}
&\int_{E_1} (u_i(x)\, \tau_{ij:k}^{GP}(x \mid x') - u_{i:k}^{GP}(x \mid x')\, \tau_{ij}(x))\, n_j^A(x)\, dx + \tfrac{1}{2}\, u_k(x') = u_k^{inc}(x')\,, \; x' \text{ on } E_1 \\
&\int_{E_1+E_2} (u_i(x)\, \tau_{ij:k}^{GU}(x \mid x') - u_{i:k}^{GU}(x \mid x')\, \tau_{ij}(x))\, n_j^B(x)\, dx \\
&\qquad + \int_F u_i(x)\, \tau_{ij:k}^{GU}(x \mid x')\, n_j^B(x)\, dx + \tfrac{1}{2}\, u_k(x') = 0 \quad , x' \text{ on } E_1,\, E_2 \text{ or } F \\
&\int_{E_2} (u_i(x)\, \tau_{ij:k}^{GP}(x \mid x') - u_{i:k}^{GP}(x \mid x')\, \tau_{ij}(x))\, n_j^C(x)\, dx + \tfrac{1}{2}\, u_k(x') = 0\,, \; x' \text{ on } E_2
\end{aligned} \tag{4}$$

where $\tau_{ij}^{GP}(x|x')$ is the Green function stress response to a point load acting in a planar infinite plate, $\tau_{ij}^{GU}(x|x')$ is the Green function stress response to a point load acting in an unbounded medium, n_j^A, n_j^B, and n_j^C are the outward normal vectors for the three constituent bodies, and F denotes the traction free surface of the joining body. Application of the boundary element method leads to a matrix equation for the evaluation of the displacements $u_i(x)$ and tractions $\tau_{ij}(x)\, n_j$ on the plate edges E_1 and E_2, and displacements $u_i(x)$ on F. Following computation of the wave fields on the plate edges, transmitted and reflected field amplitudes are obtained in the same fashion as previously described, using the far-field expression for the planar plate Green function response in Eq.(3).

COMPUTATIONAL STUDY

The formulation presented in [2] for modeling guided modes in a circular shell was encoded, and propagation behaviors were examined for a range of parameters of interest. Results first examine the effect of curvature on guided mode dispersion characteristics. The spatial frequency of a time harmonic wave field in a 3/16 inch thick aluminum shell (c_L=6094 m/s, c_T=3263 m/s) is plotted in Fig.(2) as a function of frequency over a range of 20 KHz to 400 KHz. Three modes are seen to propagate in this frequency range, identified as A0 (zero order anti-symmetric motion), S0 (zero order symmetric motion), and A1 (first order anti-symmetric motion). Figure (2a) overlays the dispersion curve for a 2 inch inner wall radius circular shell onto that of flat plate. Very little difference is observed, with only a slight difference seen at 20 KHz in the S0 mode. A similar overlay of dispersion curves for a 0.2 inch inner radius circular shell is shown in Fig.(2b). In this case, an appreciable difference in dispersion properties is noted. It is noted that the 0.2 inch inner radius is on the order of the 3/16 inch shell thickness. Figure(2) indicates that shell wall curvature has little influence on the temporal signal transport for radii of curvature substantially greater than the shell thickness.

Attention is now directed to the displacement profiles through the wall thickness for circular shell guided modes. Figure(3) plots tangential and normal displacements associated with A0 and S0 modes as a function of depth through the shell wall, computed at 100 KHz. Figures(3a,b,c) plots the A0 motion for a flat plate, 10 inch inner wall radius, and 2 inch inner wall radius, respectively. The left edge of the plot indicates motion at the inner wall, the right edge of the plot indicates motion at the outer wall. It is seen in the case of the flat plate that both the normal and tangential motions are opposite one another about the centerline of the plate, hence the anti-symmetric designation. In Figs.(3b,c), it is seen that the motions are not purely anti-symmetric about the centerline of the shell, with motions on the inner wall being greater than those at the outer wall. Similar plots of the motion profile are shown in Figs.(3d,e,f) for the S0 mode. In this case, it is seen that motion is not purely symmetric in the case of the curved shell. Normal motions are seen to be slightly larger at the inner shell wall, whereas tangential motions are seen to be slightly larger at the outer shell wall.

The observed difference in motion profiles for different curvatures has an implication for propagation in shells displaying non-uniform curvature. A mode freely propagating in a shell section of a given curvature will not transmit unaffected into the corresponding mode of a shell section with a different curvature when encountering a transition in curvature. The integral equation formulation of Eq.(2) was employed to examine the degree of mode conversion accompanying transmission at sharp transitions in curvature, via the configuration of Fig.(1a). Transmission and reflection coefficients were calculated for a 2 inch radius 90 degree bend in an otherwise flat 3/16 inch thick aluminum plate. A BEM solution to Eq.(2) was obtained which represented edge displacement and tractions by piecewise constant functions, with 15 elements prescribed over the joining edges. Computed energy reflection and transmission coefficients are presented in Fig.(4) over a range of 20 KHz to 300 KHz. It is seen that both A0 and S0 modes transmit around the 90 degree bend with little attenuation: only a small reduction in transmitted amplitude is seen at the lowest frequencies. No appreciable A0 to A0 reflection is observed, whereas a somewhat greater degree of S0 to S0 reflection is seen at the lowest frequencies. A small amount of A0 to S0 and S0 to A0 mode conversion is seen to occur on both transmission and reflection. As these energy conversions are reciprocal, a single plot representing both A0 to S0 and S0 to A0 conversion is shown. Overall, it is noted that energy lost due to

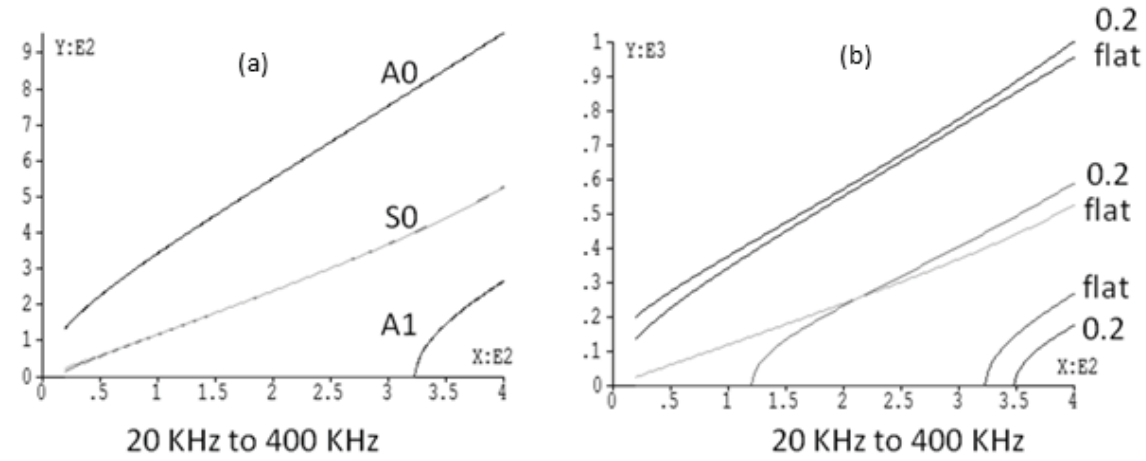

FIGURE 2. Dispersion relation for guided modes in 3/16 inch thick cylindrical shell: overlay of a) flat plate and 2 inch inner wall radius, b) flat plate and 0.2 inch inner wall radius. Vertical axis is circumferential wave number at the inner radius.

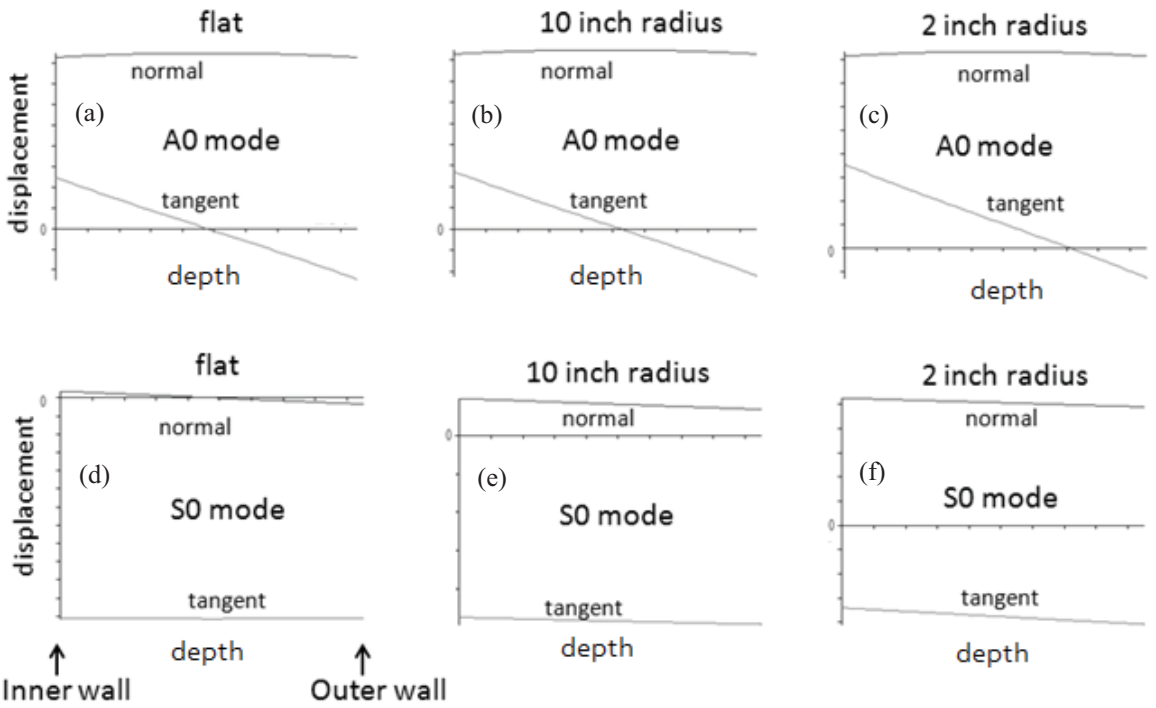

FIGURE 3. Comparison of tangential and normal 100 KHz motion profiles as function of depth through 3/16" shell wall for: a) A0 flat plate, b) A0 10 inch radius, c) A0 2 inch radius d) S0 flat plate, e) S0 10 inch radius, f) S0 2 inch radius.

mode conversion upon encountering the transition in radius is by-and-large negligible for the 2 inch radius. This result indicates that although mode conversion does occur at mild transitions in curvature, it does not have a serious deleterious effect on transmission efficiency.

Guided wave transmission in the tapered plate geometry of Fig.(1b) is modeled using the formulation expressed by Eq.(4). A doubly-curved plate section having a 2 inch inner radius connects two 3 mm semi-infinite plate sections. The thickness of the curved connecting plate section transitions from 3 mm at the interfaces with the semi-infinite plates to 6 mm at the interface between the two curved sections. An incident plate wave of either A0 or S0 motion is incident on the configuration from the left semi-infinite plate.

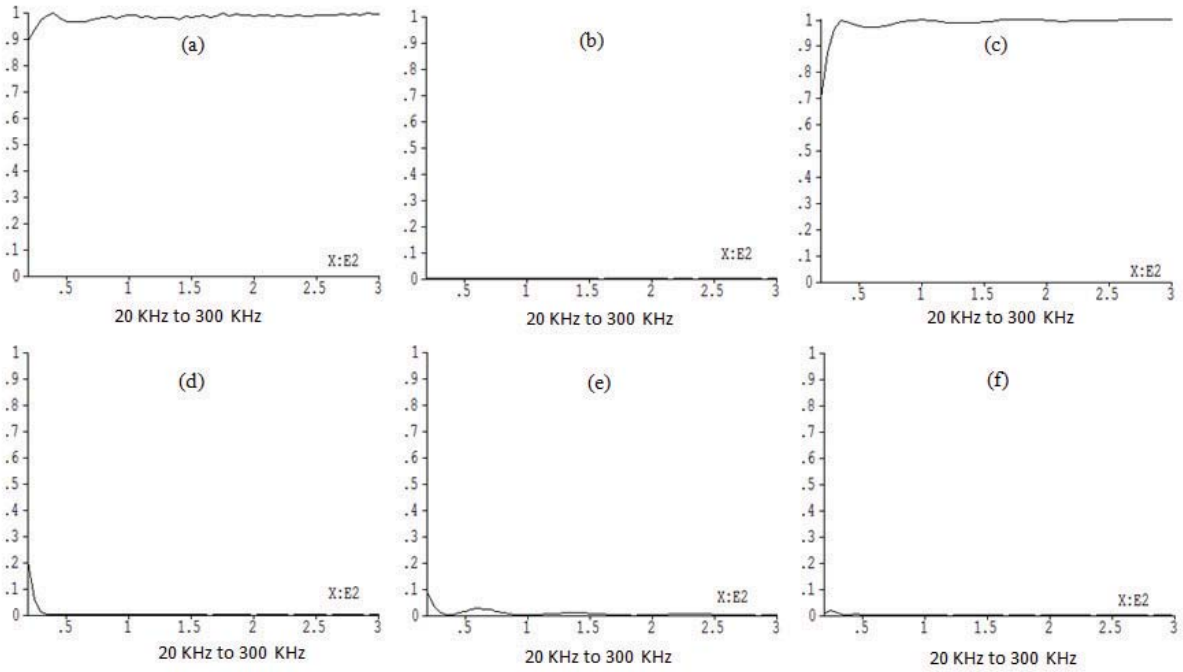

FIGURE 4. Energy transmission and reflection coefficients for: a) A0 to A0 transmission, b) A0 to A0 reflection, c) S0 to S0 transmission, d) S0 to S0 reflection, e) A0 to S0 or S0 to A0 transmission, f) A0 to S0 or S0 to A0 reflection.

Energy transmission and reflection coefficients are sought. The problem formulation of Eq.(4) is applied, and the computation is reduced to a BEM matrix equation by dividing the traction-free surfaces of the doubly-curved connecting section into 584 elements over which surface displacements are represented by piecewise constant functions. The plate edges are divided into 15 elements over which displacements and tractions are represented by piecewise constant functions, resulting in a 1288x1288 BEM matrix for inversion. Inversion of the matrix yields displacements and tractions on the plate edges joining the semi-infinite plates to the doubly-curved tapered section. Energy reflection and transmission coefficients are computed by applying Eq.(3) to the left and right semi-infinite plate sections, respectively. Results are plotted in Fig.(5) for A0 and S0 incidence between 100 KHz and 300 KHz. Figures(5a,b) plot A0 to A0 and A0 to S0 transmission. It is seen that A0 energy is transmitted by-and-large unaffected by the curved and tapered plate geometry. A small degree of A0 to S0 mode conversion is observed to occur in frequency bands around 135 KHz and 230 KHz. No appreciable reflection into either A0 or S0 modes were observed, and therefore were not plotted. Figures(5c,d) plot S0 to S0 and S0 to A0 transmission, which appear similar in behavior to A0 transmission. Notably, energy is by-and-large transmitted into a like S0 mode, with only a small degree of A0 mode coupling in frequency bands around 135 KHz and 230 KHz. Again, no appreciable A0 or S0 reflected energy was observed.

SUMMARY

Results of this study indicate that moderate degrees of plate curvature and taper have a minimal effect on the transmission efficiency of plate waves. Examination of dispersion characteristics in circular cylindrical shells revealed that the plate curvature has a negligible effect for a radius of curvature appreciably larger than the plate thickness. It was observed that displacement depth profiles vary with curvature, indicating that mode

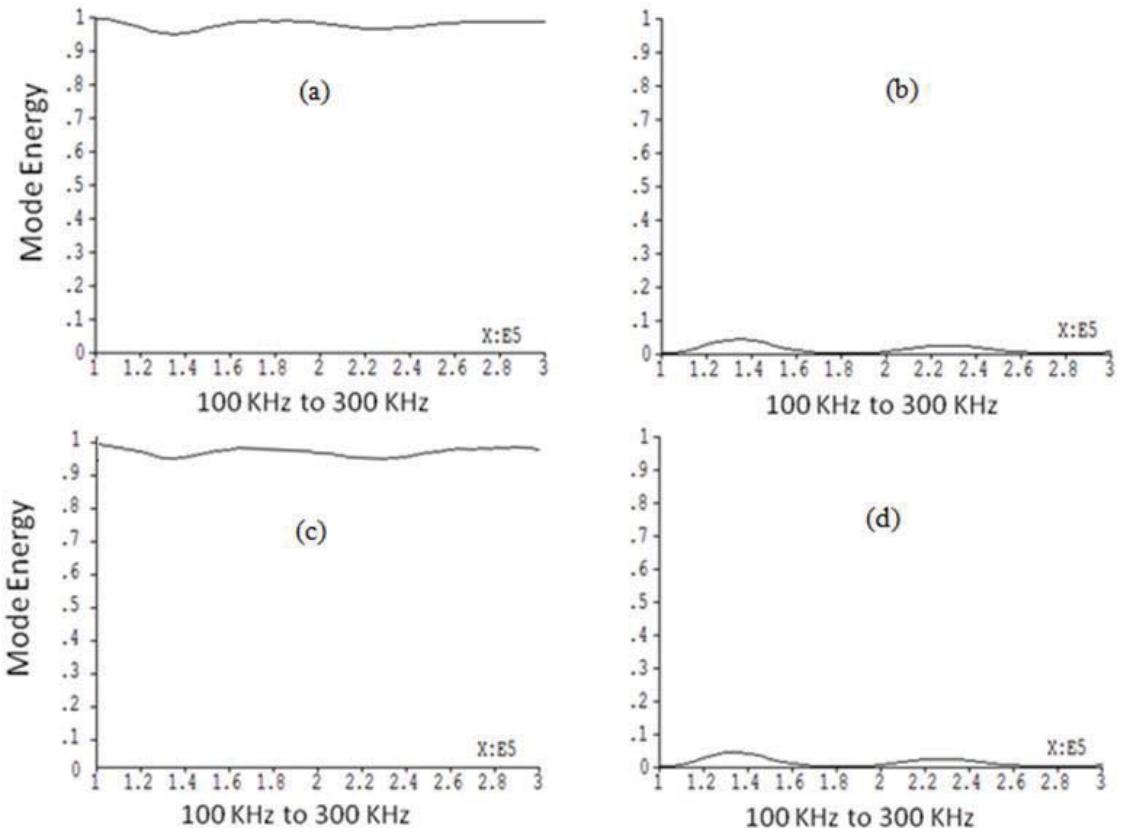

FIGURE 5. Energy transmission coefficients for configuration in Fig.(1b): a) A0 to A0, b) A0 to S0, c) S0 to S0, and d) S0 to A0. No appreciable reflection is observed.

coupling will occur when transitions in radius are encountered. However, an examination of transmission at abrupt curvature transitions revealed a negligible degree mode conversion for 3/16 inch plate radii as small as 2 inches. Finally, an examination of guided mode transmission in a curved tapered plate structure containing a two inch radius double curvature with two 100 percent transitions in thickness displayed transmission characteristics showing little mode conversion loss for both A0 and S0 wave incidence. These observations indicate that neglect of plate curvature and taper effects on plate wave transmission efficiency may under such circumstances be justified.

ACKNOWLEDGEMENT

This material is based upon work supported by the Air Force Research Laboratory under Contract # FA8650-04-C-5228 at Iowa State University's Center for NDE.

REFERENCES

1. J. Achenbach, *Wave Propagation in Elastic Solids*, Elsevier, 1982.
2. G. Liu and J. Qu, "Guided Circumferential Waves in a Circular Annulus," Trans. ASME, Vol. 65, pp. 424-430, 1998.
3. J. Achenbach, *Reciprocity In Elastodynamics*, Cambridge, UK, 2003.
4. L. Felsen and N. Marcuvitz, *Radiation and Scattering of Waves*, IEEE Press, 1994.
5. R. Roberts, "Plate Wave Transmission/Reflection at Arbitrarily Shaped Obstructions," Proceedings Review of Progress in Quantitative Nondestructive Evaluation Vol. 31, D.O. Thompson and D.E. Chimenti, Eds., AIP, N.Y., 2012.